Mirjana Puharic
Research Associate
University of Belgrade
Innovation Centre of
Technology and Metallurgy

Dusan Matic
Senior Structural Engineer
Bluewater Energy Services
Hoofddorp
Netherlands

Suzana Linic
Research Assistant
Institute Gosa, Belgrade

Slavica Ristic
Principal Researcher Fellow
Institute Gosa, Belgrade

Vojkan Lucanin
Full Professor
University of Belgrade
Faculty of Mechanical Engineering

Determination of Braking Force on the Aerodynamic Brake by Numerical Simulations

This work presents the research results of the aerodynamic brake influence, mounted on the high-speed train's roof, on the flow field and overall braking force.
The train consists of two locomotives at each end and four passenger cars between, with 121m of overall length. Aerodynamic brakes are designed to generate braking force by means of increasing the aerodynamic drag by opened panels over the train. Flow simulations were made by Fluent 12.1 software, for the train without and with one, two and three aerodynamic brakes, and velocities of 30, 50 and 70m/s. Drag force per unit panel area was determined as a function of train's velocity and the brake position. Contributions to train's gross braking force of each brake, obtained by simulations were: for first 24%, for second 15% and third 14.8%, and showed, also with panels' pressure distribution, good correlation with the aerodynamic drag calculations for flat plate orthogonally disposed to flow stream.

Keywords: *aerodynamic brake, train, aerodynamic drag.*

1. INTRODUCTION

The aerodynamic brakes, designed in the form of panels mounted over the roof of high speed train, have a task to generate the drag force by increasing the aerodynamic drag in open position. The brake that is in open position blocks the air stream and causes the overpressure appearances in front of and under-pressure behind of braking panel.

Pressure difference between in front and behind panel creates the drag force normal to the panel surface. The tangential force, the component caused by surface friction is negligibly small in comparison to normal force, which presents the braking force. As the aerodynamic drag varies with the square of velocity, the braking force of aerodynamic brakes increases in proportion to the square of velocity [1].

In this paper the train consisting of two locomotives at ends and 4 passenger wagons between them was discussed. Overall length of the train composition was L = 121m. Each locomotive was 20m long, passenger wagons the same – 20m long and the gaps between passengers wagons was 0.2m width. In Fig.1.a and 1.b, the first brake position was shown at the distance of 6m behind the train nose, and in Fig. 1.c the placement of second brake, which was placed at 17m behind the first one. The third brake was placed at a distance of 20m behind second the brake.

Flow field numerical simulations facilitate the determination of the braking force intensity generated by the aerodynamic brakes. Flow simulation was done for half-model train (in the following text named the train) by the use of ANSYS Fluent 12.1 software. Flow space around the half-model was discredited by the tetrahedral mesh. Boundary conditions were defined over the boundaries of the numerical flow model of the cuboidical shape. In the near space all over the train body, the appropriate mesh elements were placed in the zone of the boundary layer. Largeness of the boundary layer mesh element was defined upon the condition of y+ = 30 for the first mesh element row close to the train body, with adequate 20% mesh element scale increment for every other mesh element row. The number of mesh elements for the train was 5 million. Numerical flow simulations were performed for the train velocities of 30, 50 and 70m/s. Boundary conditions at the flow space input and output, in which simulations were done, were defined by the pressures at those actual positions. All other boundary conditions were defined by the flow symmetry.

Flow around the train was simulated as steady-state flow of the viscous incompressible fluid. The k – ε realizable model of turbulence was applied with standard wall functions. The average number of iterations, needed to reach the resulting convergence was about 300 [2,3].

2. THE AERODYNAMIC DRAG OF THE FLATE PLATE PLACED ORTHOGONALLY TO THE FREE STREAM

Here, the aerodynamic panels of rectangular shape, b=1.5m width and c=0.9m height, Fig. 1.b are discussed. The drag coefficient for the flat plate, with dimension ration of, was C_x=1.14 [4,5].

As well known from the aerodynamic theory, the aerodynamic drag per unit area is calculated from (1) [6]:

Received: December 2013, Accepted: February 2014
Correspondence to: Dr Mirjana Puharic
University of Belgrade, Innovation Centre of
Technology and Metallurgy, Karnegijeva 4, Belgrade
e-mail: miramo@neobee.net
doi:10.5937/fmet1402106P

$$\frac{F_x}{A} = C_X \frac{1}{2}\rho V^2 \qquad \frac{\mathrm{N}}{\mathrm{m}^2}. \tag{1}$$

Calculation results for the aerodynamic drag per flat plate unit area, for the velocities of V = 30, 50 and 70m/s, are given in the Table 1.

Table 1.

Train velocity m/s	Gross force per brakes unit area $\Delta F_x/A$ kN/m^2		
	The number of panels n		
	1	2	3
30	0.63	0.40	0.39
50	1.75	1.12	1.10
70	3.42	2.20	2.14

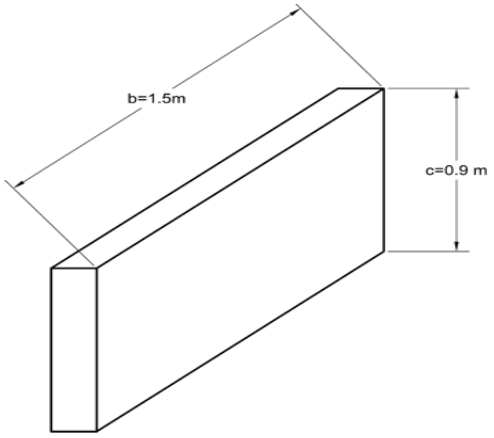

(a)

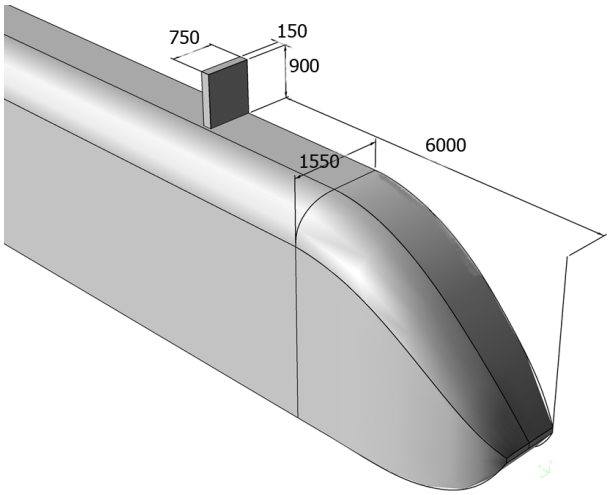

(b)

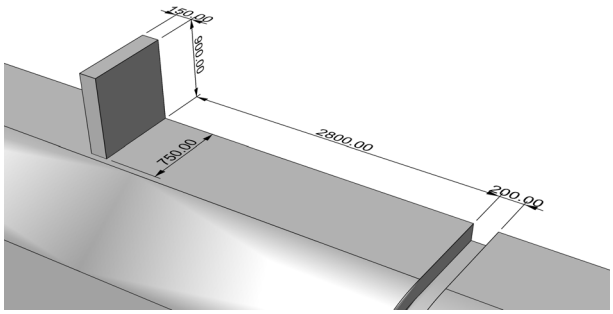

(c)

Figure 1. Train geometry and aerodynamic brakes positions

3. THE RESULTS DERIVIED BY NUMERICAL SIMULATION

In Fig. 2. the pressure distribution on the train head and the first brake is presented, under conditions of three different velocities: 30, 50 and 70m/s. At the tip zone of the train nose the over-pressure was present as well as the stagnation point. Afterwards the streamlines were accelerating and thus velocity appreciation caused pressure drop. In front the brake, the zone of high-pressure was occurring, while behind the brake the zone of low-pressure occurred because of the flow separation behind the panel. Pressure difference at the zones in front of and behind of the brake panel created drag force orthogonally to the panel surface [4, 7, 8, 9]. It could be seen that high-pressure in front of the panel was largest for the train velocity of 70m/s, as expectable.

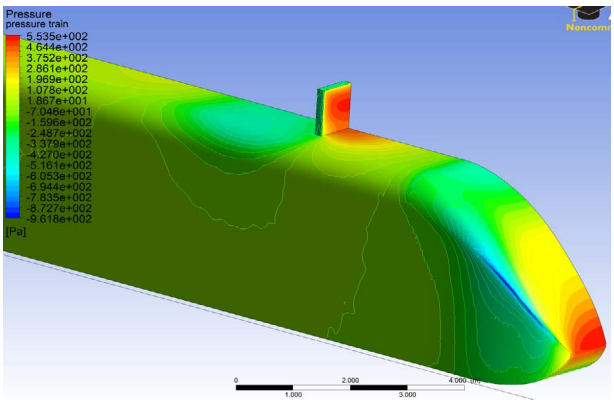

30 m/s

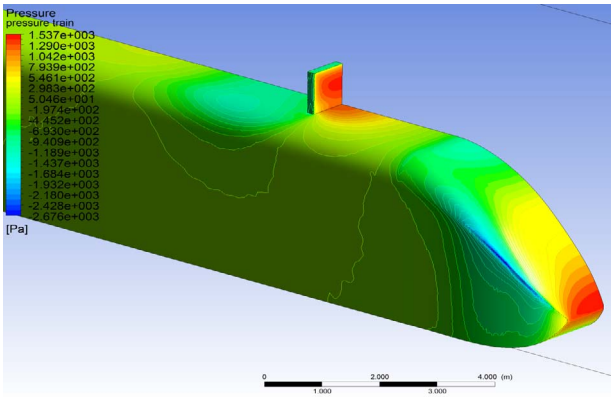

50 m/s

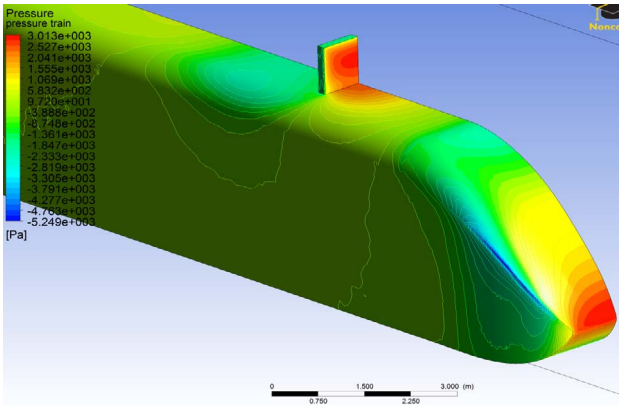

70 m/s

Figure 2. Pressure distribution at nose tip zone and on the first brake at velocities of 30, 50 and 70 m/s

Streamlines and pressure distribution over the brake at second position placed at 17m behind the first one are presented in Fig. 3. for the velocities of 30, 50 and 70m/s. In front of the brake is present a zone of high-pressure, that is lower than high-pressure value at the front side of the first brake. Behind the brake is present a zone of low-pressure that is also of lower intensity than adequate on the first brake. Streamlines are deflecting after the first brake and one part of the panel area does not contribute to the braking force. The brake at the second position was not as effective as the brake at the first position was, because it was placed inside the vortex trail made by the first brake.

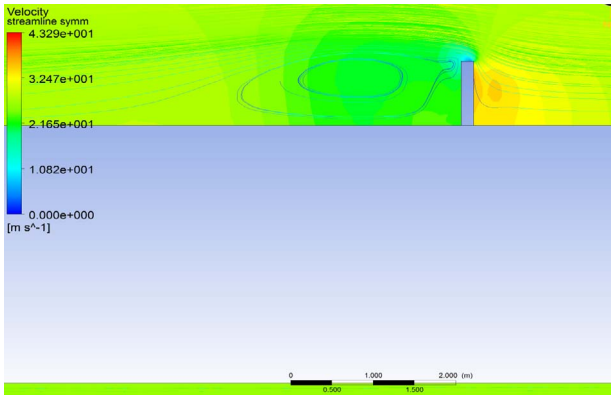

30 m/s

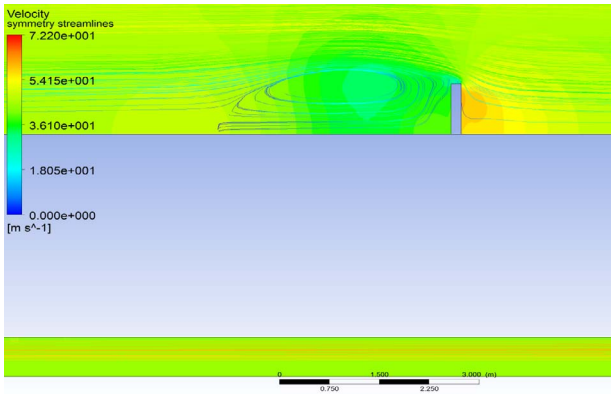

50 m/s

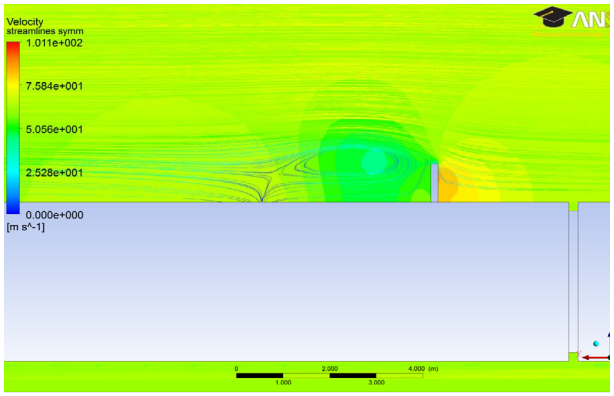

70 m/s

Figure 3. Streamline plot and the pressure distribution around second brake placed at 17m behind first brake, for the velocities of 30, 50 and 70 m/s

Streamlines and the pressure distribution around the third brake, placed at 20m behind the second one, for all three velocities, are shown in Fig. 4. Lower high-pressure values in front and the lower low-pressures values behind the third panel, were resulting in lower force per unit brake area, and therefore its weaker effectiveness.

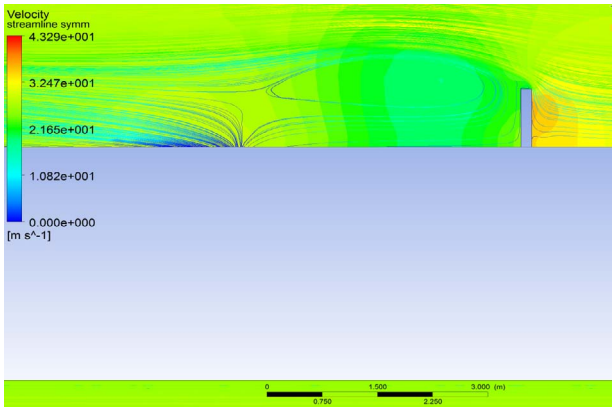

30 m/s

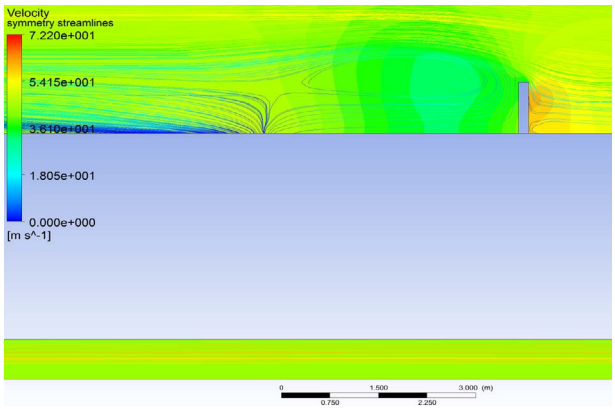

50m/s

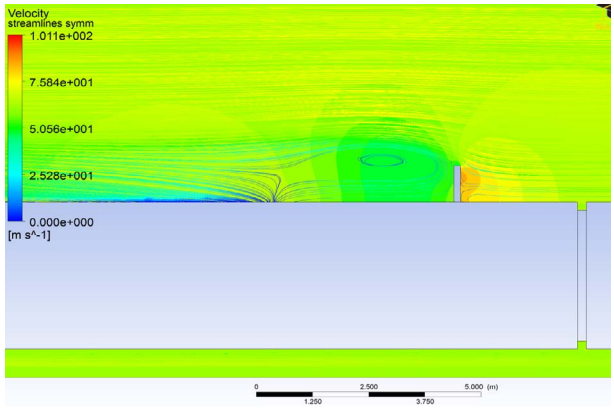

70 m/s

Figure 4. Streamline plot and the pressure distribution around the third brake, placed at 20m behind the second brake, for the velocities of 30, 50 and 70m/s

The brake placed at the first position has the largest drag, and thus it was giving the largest braking force. In Table 2. are presented the pressures in front and behind the brake panels at the first, second and third brake for all three velocities, as well as the gross force per unit area for all the three aerodynamic brakes, made by FLUENT numerical simulation. Comparison of results, calculated aerodynamic drag per unit flat plate area, given in Table 1., with the results of numerical simulation, given in Table 2., presents good output similarity.

At the brake area zone near the roof of the train, the stagnation of streamlines and recurved backward occurred, that may be noticed in Fig.3. for the velocities of 50 and 70 m/s. At that zone, the airflow pressure on the brake was largest. At the upper brake area zone, total streamline separation was occurring, and behind the brake panel the intensive vortex "bubble" was created. Thereby, the drag force was degrading rapidly. As much as brake angle of attack was larger, the "bubble" was bigger [5].

As may be seen in Fig. 3. and 4., the "bubble" has larger cross-sectional area than the brake and it was touching the roof of the train at a distance of l=k•c behind the brakes axis of rotation (where "c" was the height of the brake).

Table 2.

	Train velocity m/s								
	Number of brakes n= 1			Number of brakes n= 2			Number of brakes n= 3		
	30	50	70	30	50	70	30	50	70
Pressure in front of the brake kPa	0.423	1.12	2.4	0.297	0.666	1.5	0.225	0.65	1.45
Pressure behind the brake kPa	-0.24	-0.69	-1.2	-0.20	-0.52	-0.8	-0.19	-0.48	-0.75
Gross force per unit brake area kN/m^2	0.663	1.81	3.6	0.497	1.186	2.3	0.415	1.13	2.2

The length of intensive vortex "bubble" depended of the placement of brake and also of the train velocity and it is listed for velocities 30, 50 and 70 m/s in Table 3.

The intensive vortex "bubble" that was created behind the brake has the largest length behind the first brake. The shortest was behind the second brake, while at the third brake, the length of the "bubble" is similar to the case for the first brake.

Table 3.

Train velocity m/s	Length of the "bubble" behind the brake l=k·c		
	Number of brakes n=1	Number of brakes n=2	Number of brakes n=3
30	4,1·c	3,0·c	4,2·c
50	4,2·c	3,4·c	4,3·c
70	4,5·c	3.8·c	4,5·c

Dimension of the "bubble" is also the function of the train velocity. Comparison for the brakes on the same placement, it is noticeable that the intensive vortex "bubble" was largest for the velocity of 70m/s and it was shortest for the velocity of 30m/s.

3.1 The effect of serial interference

In case where aerodynamic brakes are placed at several positions, brake panels placed at the first positions are creating the largest drag, while for the second and third positions of brake panels the drag was decreasing, and by this means their contribution to gross braking force. This phenomenon, caused by streamline separation at the first brake, is called the effect of serial interference.

In Fig. 5., 6. and 7. streamline plots are shown in surrounding of all brakes, for the velocities of 30, 50 and 70 m/s. Figures clearly present the effect of serial interference. The streamline behind and in front the third brake is more similar to the streamline around the first brake, because the distance between the second and third brake is greater than distance between the first and the second one. Thus, the third brake was mounted at distance of 20m behind second brake. It is noticeable that streamlines were in touch again with the train roof and that the larger brake area is disposed to the act of air flow.

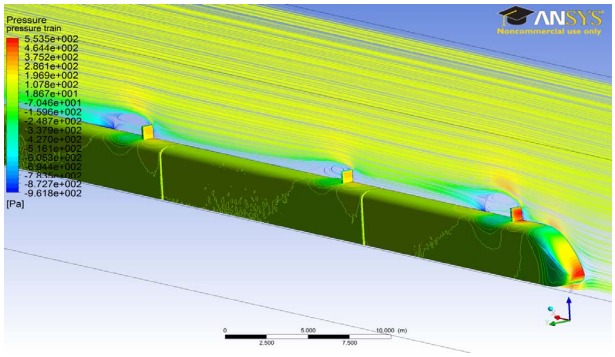

Figure 5. Streamlines around aerodynamic brakes on the train roof, at the plane of symmetry for velocity of 30m/s

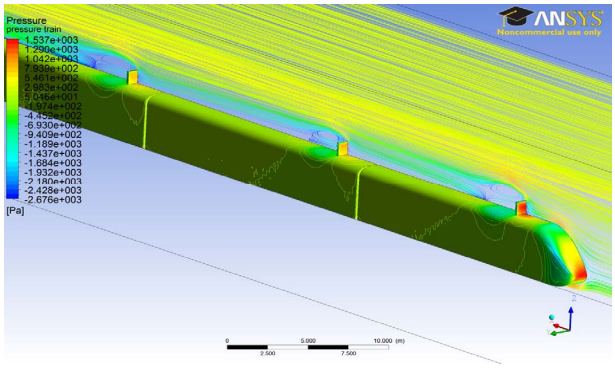

Figure 6. Streamlines around aerodynamic brakes on the train roof, at the plane of symmetry for velocity of 50m/s

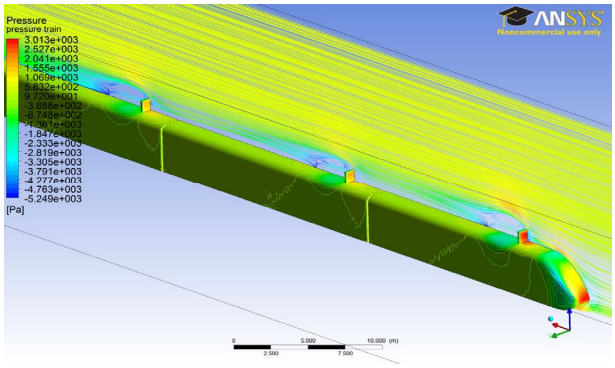

Figure 7. Streamlines around aerodynamic brakes on the train roof, at the plane of symmetry for velocity of 70m/s

It may be concluded that necessary distance between the brakes is approximately 20m, as the brake would not be placed inside the vortex airflow of front brake. The brake at the second position was placed inside the vortex trail of the first brake, because it was placed at the distance of 17 m behind the first one. This phenomenon was present for all three train velocities.

The flow between the brakes, except distances, is affected by the speed of movement, brakes' geometric shape, as well as their angle of attack [4]. Future research will be focused in this direction.

3.2 Braking force

Drag forces for clear train configuration without brakes, and for the cases with pulled out one, two and three aerodynamic brakes, is given in Table 4.

Table 4.

Train velocity m/s	Drag Force F_X kN			
	Number of brakes n			
	0	1	2	3
30	3.96	4.88	5.50	6.06
50	10.59	13.10	14.72	16.27
70	20.61	25.47	28.6	31.64

The contribution of the drag per unit area of each of the brakes to gross aerodynamic drag of the train was calculated as follows (2):

$$\frac{\Delta F_{xn}}{A_{koc}} = \frac{F_{xn} - F_{x(n-1)}}{A_{koc}} \qquad \frac{kN}{m^2}, \tag{2}$$

where :

ΔF_{xn} – the contribution of each of the brake separately to the gross train aerodynamic drag,
F_{xn} – the aerodynamic drag force of the train, when n brake panels were pulled out,
A_{koc} – the area of the aerodynamic brake panel.

In Table 5. a separate contribution of each brake to gross aerodynamic drag is shown.

Table 5.

Train velocity m/s	Contribution to drag force $\Delta F_{xn}/A_{koc}$ kN/m^2		
	Number of brakes n		
	1	2	3
30	0.68	0.46	0.41
50	1.86	1.2	1.15
70	3.6	2.32	2.25

Comparison of the results presented in Tables 1.,2. and 5. show a good correlation.

The analysis of the effect of serial interference, i.e. the influence of the first brake on the other two that are behind, can be made in the following way. Every contribution partly, of each brake, to gross train drag is equal to:

$$\frac{F_{xn} - F_{x(n-1)}}{F_{x\ bez\ koc}}.$$

The first brake's contribution is 24% to gross train drag, the second brake contributes with 15% and the third one with 14.8%, for all three velocities. This result is in correspondence with the research made for the train Maglev MLUOOl on railroad Yamanashi. By this test it was shown that the second and the other brakes, at all other positions give almost the same contribution [1].

4. CONCLUSION

The force of aerodynamic drag is proportional to the square of train velocity, thus pulling out of panels over the train can create a braking force with defined intensity that becomes more significant by increasing the train velocity. The aerodynamic brakes like those discussed can be used for trains in extremely urgent situations, when the imperative is rapid stopping.

FLUENT flow simulations, for the train configuration with two locomotives at the ends and four passenger wagons in middle, for the velocities of 30, 50 and 70 m/s, for clear train and the train with one, two and three aerodynamic brakes over the train roof, have shown that low-pressure zones were arising behind the panel and the high -pressure zone in front of the panel, resulted from the creation of the drag force on the brake. For all the three brakes, dimensions of the intensive vortex "bubble", behind the panel, was analyzed. It was noticed that the "bubble" length at the first and third brake are the same, while the "bubble" behind the second brake has shorter length. This was caused by the fact that the distance between the first and second brake was smaller than distance between the second and third one. A dimension of the "bubble" depends also of train velocity. The "bubble" was largest when the train velocity was highest (by 70m/s).

It was also showed that braking panels, placed at the first position, were creating the largest drag, while for panels at the second and other positions drag force is decreasing, and that means their contribution to the braking force. At the first brake the separation of air streamlines was occurring so the second brake was implicated by vortex trail of the first brake.

Contributions to the braking force of every single brake, obtained by FLUENT simulations and those from pressure distributions in front and behind the panel, showed good correlation of results with the aerodynamic drag calculations for flat plate, disposed orthogonally to the flow stream. Contributions of every brake to the gross braking force of observed train, were as follows for the first brake it was 24%, for the second 15% and for the third one 14.8%. These results were in correspondence with the results from tests made for the train Maglev on the Yamanashi test railway.

ACKNOWLEDGMENT

This paper is a result of research realized by the project of the Ministry of Science and Technological Development, Republic of Serbia TR-35045. Scientific-technological support to enhancing the safety of special road and rail vehicles, 2011.-2014.

REFERENCES

[1] Yoshimura, M., Saito, S., Hosaka, S. and Tsunoda H.: Characteristics of the aerodynamic brake of the vehicle on the Yamanashi Maglev test line, QR of RTRI, vol.41, No.2, jun 2000.

[2] Veersteg, H.K. and Malalasekera, W.: *An Introduction to computational fluid dynamics, The finite volume method*, Longman, 1995.

[3] Blazek, J.: *Computational Fluid Dynamics, Principles and Applications*, Elsevier, 2001.

[4] Vasović, I., Maksimović, M., Puharić, M., Matić, D. and Linić, S.: Structural analysis of aerodynamic brake of high-speed train, Scientific Technical Review, Vol.61, No 2, pp.10-15, 2011.

[5] Rendulic, Z.: *Purpose, Selection and Aerodynamic Calculation of the Aerodynamic Brakes*, Faculty of the Mechanical Engineering in Belgrade (Namena, izbor i aerodinamički proračun vazdušnih kočnica, diplomski rad, Mašinski fakultet Beograd), 1974.

[6] Anderson, J.D., *Fundamentals of aerodynamics*, McGraw-Hill, inc, 1996.

[7] Raghu, S., Raghunathan, R.S, Kim, H.-D. Setoguchi, T.: Aerodynamics of high-speed railway train, Review Article Progress in Aerospace Sciences, Vol. 38, No. 6-7, pp. 469-514, 2002.

[8] Puharić, M., Lučanin, V., Ristić, S. and Linić, S.: *Application of the Aerodynamic Brakes on Trains*, Researches and Designs for the Commerce (Primena aerodinamičkih kočnica na vozove, Istraživanja i projektovanja za privredu), ISSN 1451-4117, UDC 33, 8(2010)1, 168, pp.13-21, 2010.

[9] Puharić, M., Linić, S., Matić, D. and Lučanin, V.: Determination of braking force of aerodynamic brakes for high speed trains, Transactions of Famena XXXV-3 (2011), ISSN 1333-1124, UDC 629.4.56, UDC 629.4.077, pp. 57-66, 2011.

ОДРЕЂИВАЊЕ СИЛЕ КОЧЕЊА НА АЕРОДИНАМИЧКИМ КОЧНИЦАМА ПОМОЋУ НУМЕРИЧКИХ СИМУЛАЦИЈА

Мирјана Пухарић, Душан Матић, Сузана Линић, Славица Ристић, Војкан Лучанин

Овај рад представља резултате истраживања утицаја аеродинамичких кочница, постављених на кров брзог воза, на струјно поље и укупну силу кочења.

Воз се састоји од две локомотиве, на сваком крају, и четири путничка вагона., укупне дужине 121м. Аеродинамичке кочнице стварају силу кочења повећавањем аеродинамичког отпора помоћу извучених панела на крову воза. Симулације струјања су урађене софтвером Флуент 12.1, за воз без, са једном, две и три аеродинамичке кочнице, при брзинама од 30, 50 и 70m/s. Сила отпора по јединици површине панела је одређена као функција брзине воза и положаја аеродинамичке кочнице. Доприноси укупној сили кочења сваке од кочница, одређени симулацијама су: за прву 24%, за другу 15% и за трећу 14.8% и показали су , заједно са расподелама притисака по панелима, добро слагање са прорачунима аеродинамичког отпора за равну плочу управно постављену према струјању.